Precise all-electron dynamical response functions: Application to COHSEX and the RPA correlation energy

Markus Betzinger,[1,*] Christoph Friedrich,[1] Andreas Görling,[2] and Stefan Blügel[1]
[1]*Peter-Grünberg Institut and Institute for Advanced Simulation, Forschungszentrum Jülich and JARA, D-52425 Jülich, Germany*
[2]*Lehrstuhl für Theoretische Chemie, Universität Erlangen-Nürnberg, Egerlandstr. 3, D-91058 Erlangen, Germany*
(Received 6 August 2015; published 1 December 2015)

We present a methodology to calculate frequency and momentum dependent all-electron response functions determined within Kohn-Sham density functional theory. It overcomes the main obstacle in calculating response functions in practice, which is the slow convergence with respect to the number of unoccupied states and the basis-set size. In this approach, the usual sum-over-states expression of perturbation theory is complemented by the response of the orbital basis functions, explicitly constructed by radial integrations of frequency-dependent Sternheimer equations. To an essential extent an infinite number of unoccupied states are included in this way. Furthermore, the response of the core electrons is treated virtually exactly, which is out of reach otherwise. The method is an extension of the recently introduced incomplete-basis-set correction (IBC) [Betzinger *et al.*, Phys. Rev. B **85**, 245124 (2012); **88**, 075130 (2013)] to the frequency and momentum domain. We have implemented the generalized IBC within the all-electron full-potential linearized augmented-plane-wave method and demonstrate for rocksalt BaO the improved convergence of the dynamical Kohn-Sham polarizability. We apply this technique to compute (a) quasiparticle energies employing the COHSEX approximation for the self-energy of many-body perturbation theory and (b) all-electron RPA correlation energies. It is shown that the favorable convergence of the polarizability is passed over to the COHSEX and RPA calculation.

DOI: 10.1103/PhysRevB.92.245101 PACS number(s): 71.15.Mb, 71.15.Ap

I. INTRODUCTION

Response functions play an important role in condensed matter theory. They describe how a many-electron system reacts to an external perturbation. For example, a perturbing electric field leads to a rearrangement of the electronic charge giving rise to polarization and screening effects. Likewise, a perturbing magnetic field may induce changes in the magnetization density. The perturbation can be caused by an incoming beam of particles, e.g., photons, electrons, and neutrons. Response functions, thus, determine the spectroscopic properties of the material. Furthermore, they are central ingredients in electronic structure methods that go beyond standard Kohn-Sham (KS) density-functional theory (DFT) [1,2]. For example, the GW approximation [3–5] for the electronic self-energy as well as the electronic correlation energy within the adiabatic-connection fluctuation-dissipation theorem (ACFDT) [6,7] using the random-phase approximation (RPA) [8–10] require the calculation of the microscopic polarizability in its most general form, i.e., with full frequency and momentum dependence.

In practice, the main obstacle in calculating the polarizability is the slow convergence with respect to the basis-set size and the number of unoccupied states. It formally involves a sum over the infinite number of unoccupied states. In a practical calculation, of course, only a finite number N of states is available, which becomes a convergence parameter. In recent years, several approaches have been proposed to accelerate the convergence. The extra-polar approximation [11] replaces the unknown energies of all bands above the Nth band by a constant parameter, which allows the sum to collapse over the unknown bands, an approach that is also known as common-energy-denominator approximation (CEDA) [12] or localized Hartree-Fock method [13] in the context of the optimized-effective-potential (OEP) method [14,15]. This approach is easy to implement, but it is not parameter-free and often still shows slow convergence with respect to N. Berger *et al.* [16,17] replaced the energies of the unoccupied states, instead, by an effective-energy function, which is independent of the band index, again allowing the infinite sum to convert to a finite one. However, while in principle exact and parameter-free, the exact form of this function is not known and must be approximated. It turns out that improving the approximations quickly becomes unwieldy. As an alternative, the solution to the differential Sternheimer equation [18] in a basis set formally gives the same result as the summation over the unoccupied states, thereby avoiding the explicit summation. However, since the solution is sought in the space spanned by the orbital basis set, the slow convergence with respect to the basis-set size remains.

In two recent papers, Refs. [19] and [20], we developed an incomplete-basis-set correction (IBC) for computing the static polarizability, numerically realized in the all-electron full-potential linearized augmented-plane-wave (FLAPW) method [21–24]. The IBC solves the aforementioned problems. It does not rely on adjustable parameters or additional approximations and captures response contributions that lie outside the space spanned by the basis set. It can be pictured as a combination of the usual sum-over-states (SOS) expression of Rayleigh-Schrödinger perturbation theory and a *basis-response* term constructed from pointwise solutions to an "atomic" Sternheimer equation. The latter incorporates the contribution of the infinitely many states that are not contained in the finite SOS. Similar ideas have been formulated by Savrasov in Ref. [25] for the linear muffin-tin orbital (LMTO) method [26,27]. In addition, the IBC comprises a *Pulay term* (named after a formally similar expression used in atomic

*m.betzinger@fz-juelich.de

force calculations [28]), which corrects for deviations of the calculated eigenfunctions from the exact pointwise solutions of the KS equation. In the derivation of the IBC, we exploit the fact that all-electron methods usually employ basis functions that are adjusted to the effective potential and therefore already represent approximate solutions to the underlying KS equation. In the FLAPW method, these functions are defined inside the muffin-tin spheres centered around the atoms. Their response to a perturbation of the effective potential can be obtained by integrating the corresponding differential radial Sternheimer equation. We demonstrated [19,20] that the IBC significantly accelerates the convergence of the static polarizability in terms of both basis-set size and the number of unoccupied states.

In this paper, we extend the IBC to frequency and momentum dependent perturbations (Sec. II A) and apply it to the dynamical polarizability (Sec. II B). The improved convergence behavior is demonstrated for rocksalt barium oxide (Sec. II C). We will see that the generalized IBC enables the calculation of highly accurate dynamical polarizabilities already with a minimal LAPW basis set. The resulting polarizabilities are then employed to compute two different properties: (a) quasiparticle energies within the COHSEX approximation for the self-energy and (b) the all-electron RPA correlation energy of BaO (Sec. III).

II. INCOMPLETE BASIS-SET CORRECTION

This section is devoted to the development of the IBC for frequency and momentum dependent perturbations. The resulting equations are formally similar to the ones derived in Refs. [19] and [20] for the static case. Therefore, we recapitulate the derivation of the IBC in Sec. II A and focus specifically on the points where the mathematical formulation has to be modified to allow for the more general case. We emphasize here the conceptual idea and discuss the IBC in an intuitive manner. A detailed derivation starting from the single-particle KS equations is presented in Appendix A. Since the core states are confined to the muffin-tin (MT) spheres and calculated in terms of a spherically symmetric effective potential, the IBC enables an exact treatment of their contribution to the polarizability, which is shown in Appendix B. Section II B uses the results to define a corrected frequency and momentum dependent polarizability. We then analyze the improved convergence behavior in Sec. II C. When referring to equations of our previous papers [19] or [20] we use a prime ($'$) or a double prime ($''$), respectively. Unless otherwise noted, we employ the same notation, definitions, and units (i.e., Hartree atomic units). For simplicity, the spin index is suppressed, and we restrict the derivation to the nonrelativistic case. The numerical implementation, however, uses the corresponding scalar-relativistic equations.

A. Generalization

The polarizability describes the linear response of the electron density to perturbations of the KS effective potential. We use the functions $M_I(\mathbf{r})$ of the mixed product basis (MPB) [29–32] as a basis set for the spatial part of the perturbations. The MT MPB functions are given as a product of a radial part and a spherical harmonic $M_I(\mathbf{r}) = M_I(r)Y_{LM}(\hat{\mathbf{r}})$ with the index $I = (a,P,L,M)$, where a is the atomic index and P distinguishes between different radial functions $M^a_{PL}(r)$.

We consider a time-dependent perturbation of the form $M_I(\mathbf{r})e^{-i\omega t}$ and write the linear response of the KS single-particle wave functions $\varphi_{n\mathbf{k}}(\mathbf{r})$ as $\varphi^{(1)}_{n\mathbf{k},I}(\mathbf{r},\omega)e^{-i\omega t}$, showing the same time dependence as the perturbing field. Since the density is written in terms of the $\varphi_{n\mathbf{k}}(\mathbf{r})$, it is this response that we deal with in the following.

When representing $\varphi_{n\mathbf{k}}(\mathbf{r}) = \sum_{\mathbf{G}} z_{\mathbf{G}}(n,\mathbf{k})\phi_{\mathbf{kG}}(\mathbf{r})$ in terms of the LAPW basis $\{\phi_{\mathbf{kG}}(\mathbf{r})\}$

$$\phi_{\mathbf{kG}}(\mathbf{r}) = \begin{cases} \exp[i(\mathbf{k}+\mathbf{G})\cdot\mathbf{r}]/\sqrt{\Omega} & \text{if } \mathbf{r} \in \text{IR} \\ \sum_{lm}\sum_{p=0}^{1} A^a_{lmp}(\mathbf{k},\mathbf{G})u^a_{lmp}(\mathbf{r}_a) & \text{if } \mathbf{r} \in \text{MT}(a), \end{cases} \tag{1}$$

[Ω denotes the volume of the unit cell, $A^a_{lmp}(\mathbf{k},\mathbf{G})$ are the matching coefficients and $\mathbf{r}_a$ is the position vector relative to the MT sphere center of atom a] differentiating with respect to the potential formally produces one term where the basis functions themselves are differentiated. Through the augmentation functions $u^a_{lmp}(\mathbf{r}) = u^a_{lp}(r)Y_{lm}(\hat{\mathbf{r}})$ defined by

$$h^a_l\, ru^a_{l0}(r) = \epsilon^a_l\, ru^a_{l0}(r) \tag{2}$$

for $p = 0$ and

$$h^a_l\, ru^a_{l1}(r) = \epsilon^a_l\, ru^a_{l1}(r) + ru^a_{l0}(r) \tag{3}$$

for $p = 1$, where ϵ^a_l is a predefined energy parameter and h^a_l denotes the radial Hamiltonian $h^a_l = -\frac{1}{2}\frac{\partial^2}{\partial r^2} + \frac{l(l+1)}{2r^2} + V^a_{\text{eff},0}(r)$, the LAPW basis functions do depend on the spherically averaged effective potential $V^a_{\text{eff},0}(r)$. We can, thus, formally define a response

$$u^{a(1)}_{lmp,I}(\mathbf{r},\omega) = \sum_{l'm'} u^{a(1)}_{lmp,I,l'm'}(r,\omega)Y_{l'm'}(\hat{\mathbf{r}}), \tag{4}$$

extending the definition of Eq. ($1''$) by the frequency of the perturbation. For a purely spherical perturbation ($L = 0$), the response remains in the same lm channel: $l' = l, m' = m$. A nonspherical perturbation ($L > 0$), on the other hand, can create response contributions in other (in general more than one) $l'm'$ channels. Using time-dependent perturbation theory for degenerate states, the radial parts for $p = 0$ and $p = 1$ can be shown to obey the inhomogeneous equations

$$\begin{aligned} &\left[h^a_{l'} - \epsilon^a_l - \omega\right] ru^{a(1)}_{lm0,I,l'm'}(r,\omega) \\ &\quad = G^{Mm'm}_{Ll'l}\left[\delta_{ll'}\epsilon^{a(1)}_{l,I} - M_I(r)\right] ru^a_{l0}(r) \end{aligned} \tag{5}$$

and

$$\begin{aligned} &\left[h^a_{l'} - \epsilon^a_l - \omega\right] ru^{a(1)}_{lm1,I,l'm'}(r,\omega) \\ &\quad = G^{Mm'm}_{Ll'l}\left[\delta_{ll'}\epsilon^{a(1)}_{l,I} - M_I(r)\right] ru^a_{l1}(r) + ru^{a(1)}_{lm0,I,l'm'}(r,\omega), \end{aligned} \tag{6}$$

reproducing Eqs. ($2''$) and ($3''$) in the limit $\omega \to 0$. The linear change $\epsilon^{a(1)}_{l,I}$ of the energy parameter ϵ^a_l is given by $\langle u^a_{l0}|M_I|u^a_{l0}\rangle$. We see that it is the Gaunt coefficient $G^{Mm'm}_{Ll'l} = \int Y_{LM}(\hat{\mathbf{r}})Y^*_{l'm'}(\hat{\mathbf{r}})Y_{lm}(\hat{\mathbf{r}})d\Omega$ that couples the LM channel of the perturbation and the lm channel of the perturbed function with the resulting $l'm'$ channel of the response. Due to the selection

rules of the Gaunt coefficients, many of the terms in Eq. (4) vanish [20]. Furthermore, it is possible to solve the linear differential equations independently of m, m', and M and subsequently simply scale the solutions by the corresponding factor $G^{Mm'm}_{Ll'l}$.

In essence, Eq. (5) is the Sternheimer equation for an atomic (i.e., spherically symmetric) problem, except for the fact that the radial functions are defined only for $r \leqslant S^a$ with the MT sphere radius S^a (no atomic boundary condition). In this sense, we can interpret $u^{a(1)}_{lm0,I,l'm'}(r,\omega)$ as an "atomic solution" that takes care of the rapid variations inside the MT spheres, which cannot be captured in practice by the usual SOS expression. We will later combine this atomic solution with the SOS and in this way introduce the necessary periodic boundary condition.

The differential equations above do not determine the response $u^{a(1)}_{lmp,I,l'm'}(r,\omega)$ uniquely since we may always add a multiple of the homogeneous solution

$$\left[h^a_{l'} - \epsilon^a_l - \omega\right] r u^{a,\mathrm{hom}}_{l,l'}(r,\omega) = 0\,. \tag{7}$$

In the previous publications, we have fixed this arbitrariness by an orthogonality condition. We have found this definition to work well in the static case but not so for $\omega \neq 0$, in particular for large ω. We therefore revert to another condition, namely that the response (and its gradient) should be continuous throughout space. Since the LAPW basis functions do not depend on the effective potential in the interstitial region, this means that the response should go to zero in value and slope at the MT sphere boundary. This condition, in fact, results naturally if we differentiate the matching coefficients $A^a_{l'm'p}(\mathbf{k},\mathbf{G})$ as part of the functional derivative of Eq. (1), which produces terms that contain the functions $u^a_{l'p}(r)$ ($p = 0,1$). Hence, we have the freedom in three coefficients

$$\begin{aligned}\tilde{u}^{a(1)}_{lmp,I,l'm'}(r,\omega) = {} & u^{a(1)}_{lmp,I,l'm'}(r,\omega) + \alpha u^{a,\mathrm{hom}}_{l,l'}(r,\omega) \\ & + \beta u^a_{l'0}(r) + \gamma u^a_{l'1}(r)\end{aligned} \tag{8}$$

but only two conditions $\tilde{u}^{a(1)}_{lmp,I,l'm'}(S^a,\omega) = \tilde{u}^{a(1)\prime}_{lmp,I,l'm'}(S^a,\omega) = 0$. We resolve this ambiguity with the choice $\gamma = 0$. This choice leads to stable results up to very large imaginary frequencies and to a fast band convergence (see results below). As a rationale, note that for small ω the three radial functions $u^{a,\mathrm{hom}}_{l',l}(r,\omega)$, $u^a_{l'0}(r)$, $u^a_{l'1}(r)$ are practically linearly dependent. In fact, it can be shown that the definition of Ref. [20] is recovered in the static limit. So far, we have only discussed the augmented plane waves of the LAPW basis set. For local orbitals ($p \geqslant 2$) [33–36], we basically use the same construction principle employing the solution of Eq. (5), now with the energy parameter $\epsilon^a_{lp} \neq \epsilon^a_l$ of the local orbital.

The generalization to momentum dependent perturbations is straightforward. For a perturbation restricted to the MT sphere, the momentum dependence can be considered by a simple phase factor $e^{i\mathbf{q}\cdot\mathbf{R}}$ with the momentum vector $\mathbf{q}$ and the position vector $\mathbf{R}$ that points to the respective MT center. This corresponds to the definition of the $\mathbf{q}$ dependent MT functions $M^{\mathbf{q}}_l(\mathbf{r})$ of the MPB [29–32]. The response simply acquires the same phase factor so that, as a result, we can write the response of a basis function $\phi_{\mathbf{kG}}(\mathbf{r})$ as

$$\begin{aligned}\phi^{(1)}_{\mathbf{kG},I\mathbf{q}}(\mathbf{r},\omega) = {} & e^{i(\mathbf{k}+\mathbf{q})\cdot\mathbf{R}} \sum_{lmp} A^a_{lmp}(\mathbf{k},\mathbf{G}) \\ & \times \sum_{l'm'} \tilde{u}^{a(1)}_{lmp,I,l'm'}(|\mathbf{r}-\mathbf{R}|,\omega) \widehat{Y_{l'm'}(\mathbf{r}-\mathbf{R})}\end{aligned} \tag{9}$$

for $\mathbf{r}$ pointing into the MT sphere centered at $\mathbf{R}$. In the interstitial region the response of the basis is zero. For local orbitals, an analogous formula is used with the local-orbital index replacing $\mathbf{G}$. Linear combination with the wave-function coefficients yields $\tilde{\varphi}^{(1)}_{n\mathbf{k},I\mathbf{q}}(\mathbf{r},\omega) = \sum_{\mathbf{G}} z_{\mathbf{G}}(n,\mathbf{k}) \phi^{(1)}_{\mathbf{kG},I\mathbf{q}}(\mathbf{r},\omega)$. Just as Eq. (9), this is a Bloch function with wave vector $\mathbf{k}+\mathbf{q}$, showing that a wave function at $\mathbf{k}$ is scattered into $\mathbf{k}+\mathbf{q}$ by a $\mathbf{q}$-like perturbation. With $\tilde{\varphi}^{(1)}_{n\mathbf{k},I\mathbf{q}}(\mathbf{r},\omega)$ as a first approximation to the response of the wave function and using time-dependent Rayleigh-Schrödinger perturbation theory only for the remainder yields a result that is formally similar to the one derived in Ref. [19],

$$\begin{aligned}\varphi^{(1)}_{n\mathbf{k},I\mathbf{q}}(\mathbf{r},\omega) = {} & \sum_{n' \leqslant N} \frac{\langle \varphi_{n'\mathbf{k}+\mathbf{q}} | M^{\mathbf{q}}_I | \varphi_{n\mathbf{k}} \rangle}{\epsilon_{n\mathbf{k}} - \epsilon_{n'\mathbf{k}+\mathbf{q}} + \omega} \varphi_{n'\mathbf{k}+\mathbf{q}}(\mathbf{r}) + \int d^3r' \left[\delta(\mathbf{r}-\mathbf{r}') - \sum_{n' \leqslant N} \varphi_{n'\mathbf{k}+\mathbf{q}}(\mathbf{r}) \varphi^*_{n'\mathbf{k}+\mathbf{q}}(\mathbf{r}') \right] \tilde{\varphi}^{(1)}_{n\mathbf{k},I\mathbf{q}}(\mathbf{r}',\omega) \\ & + \sum_{n' \leqslant N} \frac{\langle \varphi_{n'\mathbf{k}+\mathbf{q}} | H - \epsilon_{n'\mathbf{k}+\mathbf{q}} | \tilde{\varphi}^{(1)}_{n\mathbf{k},I\mathbf{q}}(\omega) \rangle}{\epsilon_{n\mathbf{k}} - \epsilon_{n'\mathbf{k}+\mathbf{q}} + \omega} \varphi_{n'\mathbf{k}+\mathbf{q}}(\mathbf{r})\,,\end{aligned} \tag{10}$$

where H is the single-particle KS Hamiltonian. In particular, we can identify several terms that we already know from the static, $\mathbf{q}$ independent case: the usual SOS expression of text-book perturbation theory, the *basis-response* (BR) term, and the *Pulay* term. It is easy to verify that the last two terms vanish in the limit of an infinite, complete basis, in which case the SOS term would yield the exact result. In the practical case of a finite, incomplete basis set, the BR term specifically adds response contributions that lie outside the Hilbert space spanned by the basis set or, in fact, the set of the calculated eigenfunctions of H, which can be smaller than the basis set. These contributions come mainly from the infinite number of states that are not included in the SOS term. The sum over n' in the BR term can also be interpreted as a double-counting correction that projects out that part of the response that is already treated by the first term. The Pulay term constitutes a correction for the SOS term that arises because the calculated eigenfunctions of H in general deviate from the true physical eigenstates due to the incompleteness of the basis set.[1] We want to stress at this point that Eq. (10) is independent of

[1] We note that there is a second Pulay term for the state $\varphi_{n\mathbf{k}}$, which is, however, negligibly small for an occupied state $\varphi_{n\mathbf{k}}$.

the specifics of the used basis set, which enter only in the construction of $\tilde{\varphi}^{(1)}_{n\mathbf{k},I\mathbf{q}}(\mathbf{r},\omega)$, defined above in the framework of the FLAPW method. We are sure that a similar construction is possible in other basis sets, such as the linear muffin-tin orbital (LMTO) [26,27] or the projector augmented-wave (PAW) [37,38] method. In this sense, the IBC appears as a rather general method that has different realizations in different approaches.

Unlike what is suggested by the name *incomplete-basis-set correction*, we also obtain an accurate description of the linear response of the core states, which, in the FLAPW method, are treated independently of the valence basis set. The core states are calculated as eigensolutions of the relativistic Dirac equation with atomic boundary conditions, retaining only the spherical part of the effective potential. The energy eigenvalue results from the requirement that the solution is regular at the nucleus $r \to 0$ and that it goes to zero for $r \to \infty$. In the same manner as for the valence states, we can obtain the core-state response as the solution of a perturbed Schrödinger equation similar to Eq. (5), where we adopt a scalar-relativistic approximation. Further details are discussed in Appendix B.

B. Polarizability

The polarizability gives the linear response of the electron number density $n(\mathbf{r})$ to perturbations of the effective potential $V_{\text{eff}}(\mathbf{r})$. It can thus be defined as the functional derivative

$$\chi_s(\mathbf{r},\mathbf{r}';\omega) = \frac{\delta n(\mathbf{r},\omega)}{\delta V_{\text{eff}}(\mathbf{r}',\omega)}, \tag{11}$$

where we have used a frequency dependent formulation. Due to the time independence of the unperturbed Hamiltonian the linear response exhibits the same frequency as the perturbing field. Representing the polarizability in the MPB and using $n(\mathbf{r}) = 2\sum_{\mathbf{k}n} |\varphi_{n\mathbf{k}}(\mathbf{r})|^2$, we can write Eq. (11) as

$$\chi_{s,IJ}(\mathbf{q},\omega) = 2\sum_{\mathbf{k}}^{\text{BZ}}\sum_{n}^{\text{occ.}} \left\langle M^{\mathbf{q}}_{I}\varphi_{n\mathbf{k}}\middle|\varphi^{(1)}_{n\mathbf{k},J\mathbf{q}}(\omega) + \varphi^{(1)}_{n\mathbf{k},J\mathbf{q}}(-\omega)\right\rangle, \tag{12}$$

where the factor 2 stems from the spin summation, and the term containing $-\omega$ comes from the derivative of the complex conjugate. The generalization to the spin-polarized case is trivial. We note that the $\mathbf{k}$ summation should be understood as an integration over the Brillouin zone (BZ). In practice, the $\mathbf{k}$-point set is finite and one uses an interpolation between the points, e.g., the tetrahedron method [39]. In this case, integration weight factors must be taken into account, which we omit here for the sake of simplicity. Now, we replace $\varphi^{(1)}_{n\mathbf{k},J\mathbf{q}}(\mathbf{r},\omega)$ by the right-hand side of Eq. (10) and obtain the polarizability as the sum of three terms

$$\chi_{s,IJ}(\mathbf{q},\omega) = \chi^{\text{SOS}}_{s,IJ}(\mathbf{q},\omega) + \chi^{\text{BR}}_{s,IJ}(\mathbf{q},\omega) + \chi^{\text{Pulay}}_{s,IJ}(\mathbf{q},\omega), \tag{13}$$

which derive from the SOS, BR, and Pulay terms. The rather lengthy formulas are explicitly given in Appendix C. The SOS term corresponds to the usual Adler-Wiser expression for the polarizability [40,41]; the other two are the IBC terms. The contribution of the core states is included in the BR term. It should be pointed out that the corrected formula for $\chi_{s,IJ}(\mathbf{q},\omega)$ is asymmetric in the indices I and J. This is evident from Eq. (12), where the Ith MPB function is projected from the left, whereas the Jth function enters the IBC-corrected expression. The deviation from exact Hermiticity is usually small. The correct symmetry is reestablished in the code simply by an explicit symmetrization of the polarizability matrix. The decomposition of Eq. (13) invites us to analyze the convergence of the three terms separately. We will carry out such an analysis in the next section.

C. Performance

We analyze the convergence of the polarizability in terms of the basis-set size and the number of unoccupied states for the example of rocksalt BaO. Barium oxide was chosen as a prototypical ionic system with localized states (O2p and semicore Ba5s and 5p). Localized states are known to cause convergence problems in the conventional SOS approach due to their slowly convergent Fourier series that allows them to couple to energetically high-lying states [42]. As the noninteracting reference system, we employ the solution of a preceding DFT calculation with the PBE functional [43] for the exchange-correlation potential and a lattice constant of 10.24 a_0 (a_0 is the Bohr radius). A reciprocal cutoff radius of 4.00 a_0^{-1} for the interstitial region and an angular momentum cutoff of 10 in the MT spheres (of both elements with $S^{\text{Ba}} = S^{\text{O}} = 2.49$ a_0) is employed. The Ba 5s and 5p semicore states are described by local orbitals. For the auxiliary MPB a reciprocal cutoff of 3.30 a_0^{-1} and an angular momentum cutoff of 4 is used. The Brillouin zone is sampled by a $2 \times 2 \times 2$ $\mathbf{k}$-point set.

As a figure of merit for the accuracy of the polarizability matrix $\chi_{s,IJ}(\mathbf{q},\omega)$, we choose its trace (tr). The formalism so far applies to real and complex frequencies ω alike. Since the ACFDT-RPA correlation energy expression only involves the imaginary frequency axis, we restrict ourselves to imaginary frequencies in the following. Furthermore, we concentrate on the valence contribution to the polarizability and leave out the core contribution for the moment, which would merely lead to a constant vertical shift of the curves.

The convergence of tr $\chi_s(\mathbf{q},\omega)$ is analyzed in Fig. 1 with respect to the basis-set size for the X point of the BZ, $\mathbf{q} = (0.0,0.5,0.5)$ in internal coordinates, and three different frequencies along the imaginary axis (which are integration points of the Gauß quadrature). The size of the LAPW basis set is controlled by mainly two parameters: the reciprocal cutoff G_{cut} and the number n_{LO} of additional sets of local orbitals. Here, one set contains in total 72 functions of orbital character $s,p,\ldots,h$ ($l = 5$) for the two atom types. While $n_{\text{LO}} = 0$ corresponds to the conventional minimal LAPW basis for BaO including the 5s and 5p semicore local orbitals amounting to 276 basis functions, the basis with $n_{\text{LO}} = 6$ contains 708 functions in total.

Figure 1 shows the expected result, namely that the conventional SOS [(green) dashed curve] converges very slowly with respect to n_{LO}. The rate of convergence gets even smaller the larger the absolute value of the frequency is, revealing that this problem intensifies for the dynamical polarizability. The curve corresponding to the BR term [(blue) dotted curve] exhibits an equally slow but inverse convergence towards zero, reflecting the improved completeness of the basis

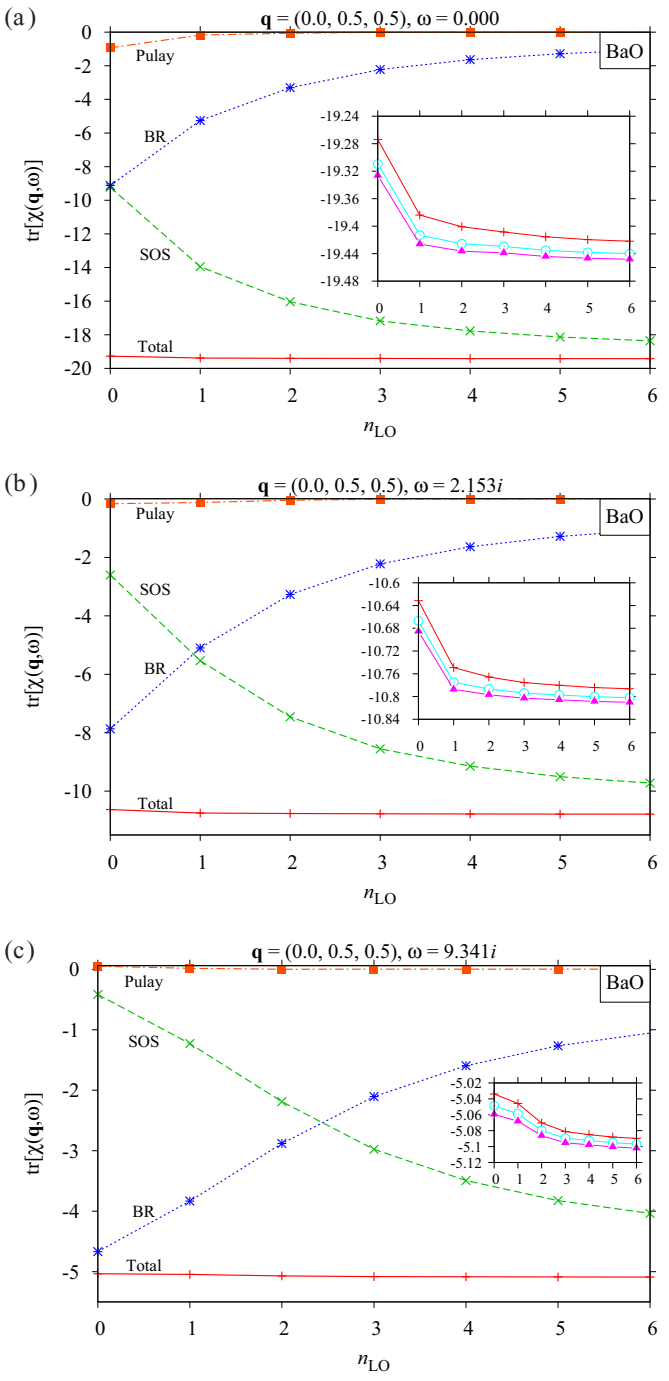

FIG. 1. (Color online) Trace of the polarizability matrix $\chi_{s,IJ}(\mathbf{q},\omega)$ for $\mathbf{q} = (0.0,0.5,0.5)$ and three different imaginary frequencies as a function of the basis-set size, indicated by n_{LO}; 276 and 708 basis functions for $n_{\mathrm{LO}} = 0$ and 6, respectively. The SOS part is shown as a (green) dashed curve and the BR and Pulay terms as (blue) dashed and (orange) dot-dashed curves, respectively. The sum of the three contributions is the IBC result and is shown as the (red) solid line. The insets show the IBC-corrected curve on a finer scale [(red) pluses], additionally for $G_{\mathrm{cut}} = 4.40\ \mathrm{a}_0^{-1}$ [(turquoise) open circles] and $4.80\ \mathrm{a}_0^{-1}$ [(magenta) filled triangles].

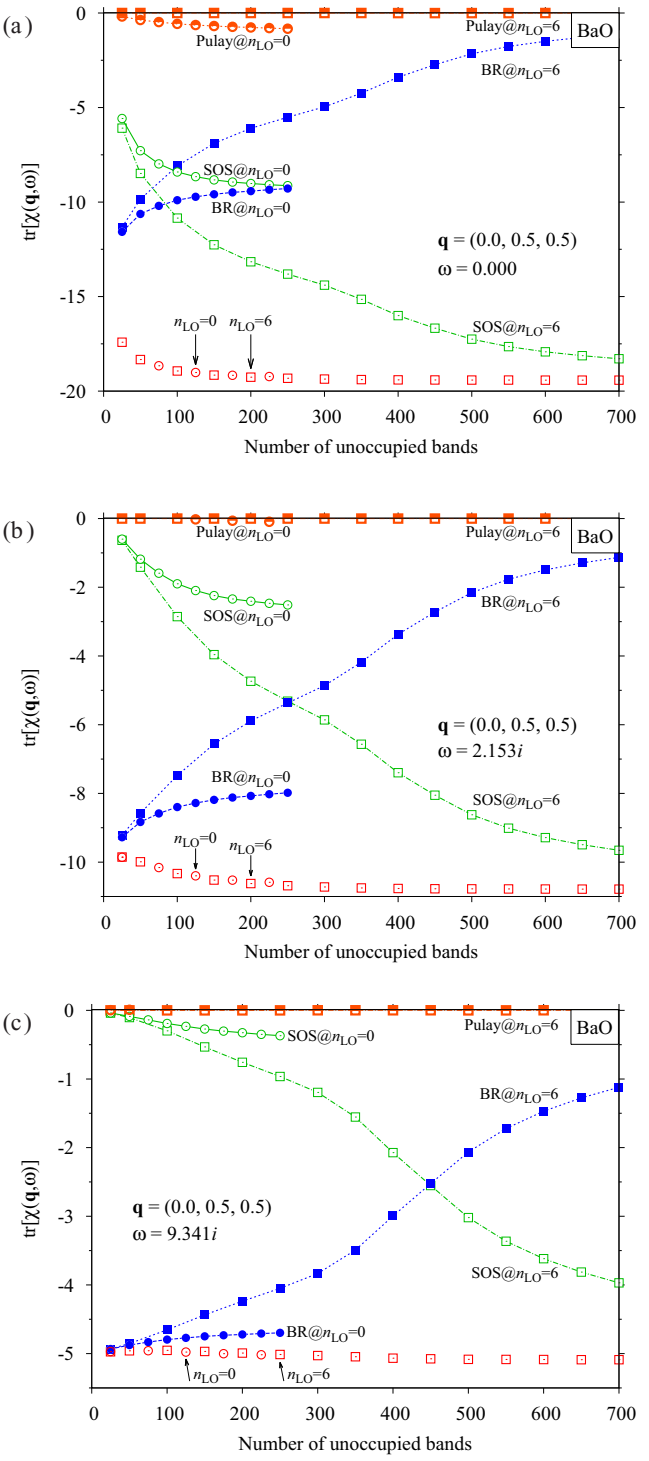

FIG. 2. (Color online) Convergence of the trace of $\chi_{s,IJ}(\mathbf{q},\omega)$ for $\mathbf{q} = (0.0,0.5,0.5)$ and three different imaginary frequencies with respect to the number of unoccupied states, for two basis sets containing 276 ($n_{\mathrm{LO}} = 0$, circles) and 708 functions ($n_{\mathrm{LO}} = 6$, squares), respectively. Green open symbols correspond to the SOS, blue filled symbols to the BR, and orange half-filled symbols to the Pulay term. The sum, given as red open symbols, shows rapid convergence independently of the chosen basis set.

set with increasing n_{LO}. When comparing the curves for the three frequencies, we observe that the BR term takes over more and more of the response for larger frequencies and, thus, compensates for the slow convergence of the SOS. The Pulay term [(orange) dot-dashed curve] gives a relatively small contribution, but still an important one for the conventional

basis set ($n_{\mathrm{LO}} = 0$), in particular for small frequencies. Adding up all three contributions yields the red curve, which is nearly a constant on the scale of the graph. The variation between $n_{\mathrm{LO}} = 0$ and $n_{\mathrm{LO}} = 6$ lies below 1.5% as can be seen in the insets, where we also show the convergence of tr $\chi_{\mathrm{s},IJ}(\mathbf{q},\omega)$ with respect to the reciprocal cutoff G_{cut}. Increasing G_{cut} to 4.40 a_0^{-1} and 4.80 a_0^{-1} changes the curves only marginally. In conclusion, the IBC enables a calculation of the dynamical polarizability that is by orders of magnitude more accurate than with the conventional SOS expression. In particular, even with the minimal LAPW basis set ($n_{\mathrm{LO}} = 0$), the polarizability is converged to an accuracy that cannot be achieved with the much larger $n_{\mathrm{LO}} = 6$ basis set without the IBC.

So far, we have included all eigenstates of the single-particle Hamiltonian in the calculation of $\chi_{\mathrm{s},IJ}(\mathbf{q},\omega)$ meaning that the number N of states used in Eq. (10) is identical to the number of basis functions. However, each of the terms in this equation depends on N. The dependence is such that the omission of bands in the SOS term will increase the BR term because a smaller portion of $\tilde{\varphi}^{(1)}_{n\mathbf{k},I\mathbf{q}}(\mathbf{r},\omega)$ is projected out. One can hope that the latter will compensate the omissions in the former so that much fewer unoccupied states are needed for convergence. This, in fact, works surprisingly well as we show in Fig. 2 for the minimal ($n_{\mathrm{LO}} = 0$) and largest ($n_{\mathrm{LO}} = 6$) LAPW basis. The figure demonstrates that the SOS term alone again converges very slowly. We note that the calculation with $n_{\mathrm{LO}} = 0$ appears to converge but to the wrong value. Adding BR and Pulay terms to the SOS yields the curve formed by the (red) open circles and squares, which exhibits a very rapid convergence with respect to the unoccupied states. Interestingly, the converged value hardly depends on the basis set used in contrast to what we find for the conventional SOS calculation. The Pulay term is again relatively small. However, for $n_{\mathrm{LO}} = 0$ and small frequencies it does give a numerically important contribution that is crucial in guaranteeing the basis-set independence of the converged polarizability.

In the form of Eq. (13), the IBC is a noniterative correction. The Pulay term gives rise to a substantial computational overhead. Instead of calculating this term explicitly, it is often a more efficient strategy to simply use one extra set of local orbitals, i.e., $n_{\mathrm{LO}} = 1$, in which case the Pulay term reduces to practically zero and does not have to be evaluated. The BR term, on the other hand, can be implemented in a rather efficient way that scales with the third power of the system size. This has to be compared to the fourth power scaling of the standard SOS term. Thus, with increasing system size the relative computational effort for calculating the BR term will decrease.

III. APPLICATIONS

The IBC, as derived in the last section, improves the convergence of the polarizability considerably. Any method that requires the knowledge of the polarizability will benefit from the correction. In the previous papers, we have applied the IBC to the optimized effective potential method [19,20,44], in which only the $\omega \to 0$ and $\mathbf{q} \to \mathbf{0}$ limit is needed. In the present paper, we have extended the formulation to momentum and frequency dependent perturbations. As practical examples, we apply the IBC to barium oxide to calculate (a) selected electronic transition energies in the COHSEX approximation for the self-energy and (b) the RPA correlation energy. While for COHSEX only the static momentum-dependent IBC is required, we need the polarizability with full momentum and frequency dependence in the case of the RPA correlation energy.

A. COHSEX

The COHSEX approximation is the static limit of the GW self-energy [3–5]. It can be divided into a screened-exchange (SEX) term Σ_{SEX} and a Coulomb-hole (COH) part Σ_{COH}:

$$\Sigma_{\mathrm{SEX}}(\mathbf{r},\mathbf{r}') = -\sum_{n\mathbf{k}}^{\mathrm{occ.}} \varphi_{n\mathbf{k}}(\mathbf{r}) W(\mathbf{r},\mathbf{r}';0) \varphi^*_{n\mathbf{k}}(\mathbf{r}') \tag{14}$$

$$\Sigma_{\mathrm{COH}}(\mathbf{r},\mathbf{r}') = \frac{1}{2}\delta(\mathbf{r}-\mathbf{r}')[W(\mathbf{r},\mathbf{r}';0) - v(\mathbf{r},\mathbf{r}')]\,. \tag{15}$$

Equation (14) has the same functional form as the Hartree-Fock exchange term with the bare Coulomb interaction $v(\mathbf{r},\mathbf{r}')$ replaced by the static limit of the RPA screened Coulomb interaction $W(\mathbf{q}) = [1 - v(\mathbf{q})\chi_{\mathrm{s}}(\mathbf{q})]^{-1} v(\mathbf{q})$. The COH term corresponds to half of the potential felt by an electron at $\mathbf{r}$ caused by the Coulomb hole around it. We restrict ourselves to first-order perturbation theory, in which the quasiparticle energies are given by $\epsilon^{\mathrm{COHSEX}}_{n\mathbf{k}} = \epsilon^{\mathrm{DFT}}_{n\mathbf{k}} + \langle\varphi_{n\mathbf{k}}|\Sigma_{\mathrm{SEX}} + \Sigma_{\mathrm{COH}} - V_{\mathrm{xc}}|\varphi_{n\mathbf{k}}\rangle$. The contribution of the core states is calculated on the Hartree-Fock level as is common practice in GW calculations. We use here the static limit of the GW self-energy, because the latter would require, in addition to the IBC-corrected W, a corresponding correction for the Green function G, which goes beyond the scope of the present study.

Barium oxide is a semiconductor with a direct band gap at the X point of the Brillouin zone. In Table I, we show the convergence of the direct band gap as well as the transition energies from the valence-band maximum to the lowest conduction states at Γ and L for different LAPW basis sets, distinguished by n_{LO} (for a definition of n_{LO} see above). We compare with the standard semilocal PBE functional [43] for the exchange-correlation energy.

The PBE functional underestimates the band gap with respect to experiment. Application of COHSEX opens the band gap, but it overshoots. The calculated band gap is nearly 2 eV larger than the experimental value. It is well known [45,46] that COHSEX shows such a tendency. We observe that the conventional calculations using the SOS exhibit a very slow convergence. On the contrary, employing the IBC in the calculation of W yields COHSEX transition energies that converge as fast as in the PBE approach. In particular, the small changes in the transition energies between $n_{\mathrm{LO}} = 1$ and $n_{\mathrm{LO}} = 0$ are merely a basis-set effect that is the same order of magnitude in the two methods. Between $n_{\mathrm{LO}} = 1$ and $n_{\mathrm{LO}} = 6$, the IBC-corrected COHSEX values are very stable; they change by maximally 4 meV, while the uncorrected values show variations that are a hundred times larger.

So far, we have restricted the IBC to response contributions from the valence bands. However, as discussed above and in more detail in Appendix B, the IBC allows us to treat the core-state response in a very precise way. Interestingly, including the core states affects the COHSEX transition energies relatively

TABLE I. PBE and COHSEX band transition energies (in eV) for rocksalt BaO as a function of the basis-set size (parameter n_{LO}) and comparison to experiment. COHSEX energies are shown without (SOS) and with the IBC. The Brillouin zone is sampled by a $4 \times 4 \times 4$ **k**-point set.

	$X_{5'v} \rightarrow X_{3c}$			$X_{5'v} \rightarrow \Gamma_{1c}$			$X_{5'v} \rightarrow L_{2'c}$		
	PBE	COHSEX@PBE		PBE	COHSEX@PBE		PBE	COHSEX@PBE	
BaO		SOS	IBC		SOS	IBC		SOS	IBC
$n_{\mathrm{LO}} = 0$	1.808	4.401	6.017	4.239	6.699	8.162	5.044	7.873	8.766
$n_{\mathrm{LO}} = 1$	1.793	5.456	5.930	3.888	7.318	7.709	5.014	8.402	8.637
$n_{\mathrm{LO}} = 2$	1.793	5.777	5.927	3.881	7.585	7.709	5.012	8.564	8.635
$n_{\mathrm{LO}} = 3$	1.793	5.878	5.926	3.881	7.669	7.706	5.012	8.611	8.635
$n_{\mathrm{LO}} = 4$	1.793	5.906	5.926	3.880	7.693	7.706	5.012	8.625	8.635
$n_{\mathrm{LO}} = 5$	1.793	5.916	5.926	3.880	7.700	7.706	5.012	8.630	8.635
$n_{\mathrm{LO}} = 6$	1.793	5.920	5.926	3.880	7.704	7.706	5.012	8.632	8.635
Expt.		3.9[a],4.1[b]							

[a]Reference [47].
[b]Reference [48].

strongly. The direct band gap changes to 6.08 eV. For the $X_{5'v} \rightarrow \Gamma_{1c}$ and $X_{5'v} \rightarrow L_{2'c}$ we obtain 7.46 eV and 8.72 eV, respectively. We find that it is the COH term that is responsible for these changes, while the SEX term is insensitive to the response coming from the core states. This is reminiscent of the fact that the COH term is known to overestimate the contribution of high-lying bands [46], because it assumes the energies of the relevant bands to be close to each other. The same seems to hold for the core states; while they do give a sizable response contribution, the COHSEX approximation exaggerates the effect as it does not take the energy distance between the core and valence states properly into account.

B. RPA correlation energy

Based on the ACFDT [6,7], the exchange-correlation energy of KS DFT can be represented exactly in terms of the dynamical polarizability of the interacting (scaled) electron system. Applying the random-phase approximation (RPA) for the interacting response then yields the RPA correlation energy

$$E_{\mathrm{c}}^{\mathrm{RPA}}[n] = \frac{1}{2\pi} \sum_{\mathbf{q}}^{\mathrm{BZ}} \int_0^\infty \mathrm{tr}\{\ln[1 - v(\mathbf{q})\chi_{\mathrm{s}}(\mathbf{q},i\omega)] + v(\mathbf{q})\chi_{\mathrm{s}}(\mathbf{q},i\omega)\} d\omega\,, \tag{16}$$

where all quantities in the trace (tr) are understood as matrices: the unit matrix 1 with the elements δ_{IJ}, the polarizability matrix $\chi_{\mathrm{s},IJ}(\mathbf{q},i\omega)$ evaluated at the imaginary frequency $i\omega$, and the matrix $v_{IJ}(\mathbf{q})$ representing the bare Coulomb interaction in the MPB. Exploiting the invariance of the trace under cyclic permutations, the matrix in the curly brackets can be replaced by the symmetrized expression $\ln[1 - A(\mathbf{q},i\omega)] + A(\mathbf{q},i\omega)$ with $A(\mathbf{q},i\omega) = v^{1/2}(\mathbf{q})\chi_{\mathrm{s}}(\mathbf{q},i\omega)v^{1/2}(\mathbf{q})$, which allows us to calculate the trace by $\sum_j \ln[1 - a_j(\mathbf{q},i\omega)] + a_j(\mathbf{q},i\omega)$ with the eigenvalues $a_j(\mathbf{q},i\omega)$ of $A(\mathbf{q},i\omega)$. Further details of the implementation will be published elsewhere [49].

In Fig. 3, we show the convergence of the RPA correlation energy for BaO. According to the band summation in Eq. (12), we define a valence-only (i.e., n is restricted to the valence states) and an all-electron (i.e., n runs over the core states in addition) polarizability, which after insertion into Eq. (16) yields a valence-only (left axis) and an all-electron (right axis) RPA correlation energy. To see the effect of the IBC, we

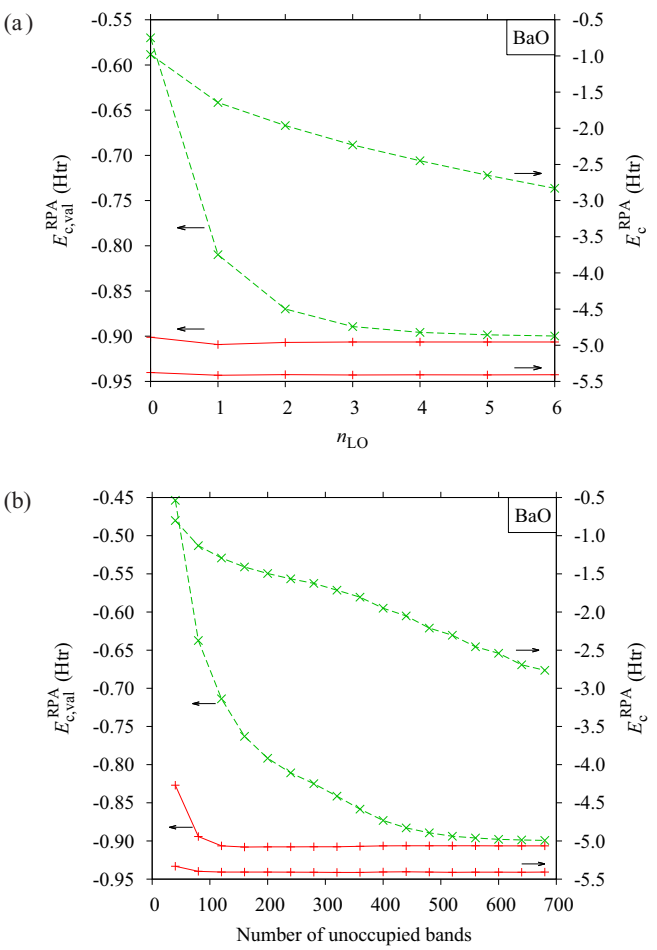

FIG. 3. (Color online) Convergence of the valence-only (left axis) and all-electron (right axis) RPA correlation energy for BaO with respect to (a) the basis-set size (parameter n_{LO}) and (b) the number of unoccupied states without (green dashed lines) and with IBC (red solid line) for a LAPW basis with $n_{\mathrm{LO}} = 6$.

also distinguish between a calculation without the correction [i.e., using only the standard SOS term of Eq. (13)] and the full expression including the BR and the Pulay terms. The RPA correlation energy clearly benefits from the improved convergence behavior of the polarizability when the IBC is employed. While the valence correlation energy does eventually converge when local orbitals are added to the LAPW basis [Fig. 3(a)], this appears to be impossible for the all-electron energy calculated with the SOS term alone. It is clear that the latter is incapable of yielding the correct contribution of the core states to the RPA correlation energy. Even with the largest basis set ($n_{\mathrm{LO}} = 6$) it is off by a factor. With the IBC, on the other hand, valence-only and all-electron correlation energies are converged for all practical purposes already with the conventional minimal LAPW basis, convincingly shown by the near constancy of the solid line. We also find again a very fast convergence with respect to the number of unoccupied states shown in Fig. 3(b).

The contribution of the core electrons to the absolute correlation energy is dominant. It amounts to about -4.5 Htr and accounts for 83% of the all-electron RPA correlation energy of BaO. Interestingly, this ratio is close to the percentage (75%) of core electrons (48) to the total number of electrons (64), so that each electron of the system, valence and core, seems to contribute a comparable amount. This is not surprising if one remembers that the leading term of the LDA correlation energy (in the low-density limit) is an integral over $n(\mathbf{r})^{4/3}$. The power $4/3$ is reasonably close to 1, in which case the contribution per occupied state would in fact be a constant. It is also known from quantum chemical calculations that the core electrons yield a substantial contribution to the correlation energy and that it is not justified to neglect them when absolute energies are needed [50].

IV. CONCLUSIONS

In this paper, we have presented a technique to compute precise frequency and momentum dependent all-electron response functions. It constitutes a generalization of the recently introduced incomplete-basis-set correction (IBC) [19,20]. In this approach, the response of the basis functions used to represent the single-particle orbitals is explicitly constructed by radial integration of frequency-dependent Sternheimer equations and combined with the sum-over-states expression of standard perturbation theory. In this way, response contributions that lie outside the Hilbert space spanned by the original basis are taken into account. The total response then consists of three terms: the sum-over-states expression of conventional perturbation theory, a basis-response term, and a Pulay term. While the basis-response term incorporates to some extent an infinite number of states, the Pulay term corrects for deviations of the single-particle wave functions calculated in the finite orbital basis from the exact pointwise solutions of the Hamiltonian.

We demonstrated within the all-electron FLAPW approach that the IBC substantially improves the convergence of the frequency- and momentum-dependent polarizability in terms of both basis-set size and number of unoccupied states. A highly converged response is already obtained with a minimal LAPW basis set. With increasing frequency, we observed that the IBC becomes even more important because the LAPW basis turns out to be less and less adequate to describe the dynamical response. In addition, the IBC enables a virtually exact treatment of the core-electron response, which is otherwise out of reach.

Any method that involves a response function directly benefits from the IBC. For example, we have utilized the IBC to compute quasiparticle energies of BaO in the COHSEX approximation for the electronic self-energy, which requires the momentum-dependent static polarizability. Thanks to the IBC, the calculations exhibit a basis-set convergence that is as fast as in DFT calculations using standard local or semilocal exchange-correlation functionals. A combination of the IBC with the recently published modified static remainder approach [51] seems promising to improve the convergence of GW calculations. While the modified static remainder approach accelerates the convergence of G, the IBC addresses the convergence of W.

As a second application, we have applied the IBC to calculate the RPA correlation energy of BaO, whose central ingredient is the frequency- and momentum-dependent polarizability. The favorable convergence of the polarizability is directly transferred to the RPA correlation energy. We showed that, when absolute correlation energies are needed, the contribution of the core electrons is not negligible. In fact, their individual contribution is comparable to that of the valence electrons. The IBC thus paves the way for the computation of truly all-electron RPA correlation energies.

The IBC, as formulated in the present paper, is applicable foremost to electronic structure methods with an explicit potential-dependent basis set, such as the LAPW or the LMTO approach. However, we believe that similar corrections could be constructed for other basis sets as well, most obviously for pretabulated numeric atomic basis sets, but also for plane-wave based methods, given that a plane wave is the eigenfunction to the Schrödinger equation with a constant effective potential and so, in this sense, also potential adjusted.

ACKNOWLEDGMENTS

M.B. acknowledges valuable discussions with Marcel Gurris, Gregor Michalicek, and Daniel Aaron Klüppelberg as well as financial support from the Helmholtz Association through the Helmholtz Postdoc Programme (VH-PD-022). A.G. is grateful for support by the DFG through Grant No. G0 523/14-1 and the collaborative research center SFB 953.

APPENDIX A: GENERALIZATION TO FREQUENCY-DEPENDENT PERTURBATIONS

In order to derive the IBC for frequency-dependent perturbations we start from the time-dependent Schrödinger equation for the one-particle orbital $\varphi_n(\mathbf{r},t)$

$$[i\,\partial_t - H]\varphi_n(\mathbf{r},t) = 0\,, \tag{A1}$$

where the Hamiltonian H is assumed to be time independent and n is a multi-index comprising a full set of quantum numbers to uniquely specify the orbital. We assume that the wave functions $\varphi_n(\mathbf{r},t)$ are represented by a (explicit)

time-independent basis set $\{\phi_j(\mathbf{r})\}$

$$\varphi_n(\mathbf{r},t) = \sum_j z_j(n,t)\phi_j(\mathbf{r}), \tag{A2}$$

and that the basis functions $\phi_j(\mathbf{r})$ are adjusted to the potential of the Hamiltonian H as is common practice in all-electron electronic structure methods.

The expansion coefficients $z_j(n,t)$ then result from the algebraic equation

$$\sum_j \langle\phi_k|i\,\partial_t - H|\phi_j\rangle z_j(n,t) = 0. \tag{A3}$$

For the time-independent Hamiltonian H the time-dependent expansion coefficients $z_j(n,t)$ are simply given by

$$z_j(n,t) = z_j(n)\exp(-i\epsilon_n t), \tag{A4}$$

where $z_j(n)$ denotes the eigenvector of the general eigenvalue problem

$$\sum_j \langle\phi_k|\epsilon_n - H|\phi_j\rangle z_j(n) = 0 \tag{A5}$$

with eigenvalue ϵ_n and overlap matrix $\langle\phi_k|\phi_j\rangle$. The latter arises from the nonorthogonality of the basis functions.

Subjecting the system to a time-dependent perturbation $W(t)$ will cause a change in the expansion coefficients $z_j(n,t)$, and moreover the assumed potential dependence of the basis functions $\phi_j(\mathbf{r})$ induces a time-dependent change of the basis. Consequently, the first order change of the wave function $\varphi_n^{(1)}(\mathbf{r},t)$ consists of two contributions

$$\varphi_n^{(1)}(\mathbf{r},t) = \sum_j z_j^{(1)}(n,t)\phi_j^{(0)}(\mathbf{r}) + z_j^{(0)}(n,t)\phi_j^{(1)}(\mathbf{r},t). \tag{A6}$$

The superscript (0) and (1) distinguish between unperturbed and perturbed quantities.

For a more compact notation of the wave-function response we introduce the abbreviations

$$\hat{\varphi}_n^{(1)}(\mathbf{r},t) = \sum_j z_j^{(1)}(n,t)\phi_j^{(0)}(\mathbf{r}) \tag{A7}$$

$$\tilde{\varphi}_n^{(1)}(\mathbf{r},t) = \sum_j z_j^{(0)}(n,t)\phi_j^{(1)}(\mathbf{r},t), \tag{A8}$$

which correspond to Eq. (24′). The exact form of the basis-function response $\phi_j^{(1)}(\mathbf{r},t)$ depends of course on the specifics of the underlying electronic structure method. For the moment, however, we assume that the response of the basis functions $\phi_j^{(1)}(\mathbf{r},t)$ is known and thereby $\tilde{\varphi}_n^{(1)}(\mathbf{r},t)$ is completely fixed. The remaining unknown is the first-order change of the expansion coefficient $z_j^{(1)}(n,t)$, which we will determine in the following.

Linearizing Eq. (A3) with respect to the potential and taking into account the change of the expansion coefficient as well as the change of the basis function according to Eq. (A6) leads to the following set of equations for the coefficients $z_j^{(1)}(n,t)$:

$$\begin{aligned}
&\left[i\langle\phi_k^{(0)}|\phi_j^{(0)}\rangle\partial_t - \langle\phi_k^{(0)}|H|\phi_j^{(0)}\rangle\right]z_j^{(1)}(n,t)\\
&\quad= \left[\langle\phi_k^{(0)}|W|\phi_j^{(0)}\rangle + \langle\phi_k^{(0)}|H|\phi_j^{(1)}\rangle + \langle\phi_k^{(1)}|H|\phi_j^{(0)}\rangle\right]z_j^{(0)}(n,t)\\
&\qquad - i\left[\langle\phi_k^{(1)}|\phi_j^{(0)}\rangle + \langle\phi_k^{(0)}|\phi_j^{(1)}\rangle\right]\partial_t z_j^{(0)}(n,t)\\
&\qquad - i\, z_j^{(0)}(n,t)\langle\phi_k^{(0)}|\partial_t\phi_j^{(1)}\rangle.
\end{aligned} \tag{A9}$$

By Fourier transforming all time-dependent quantities to the frequency domain, the set of coupled differential equations in time turns into a set of algebraic equations

$$\begin{aligned}
&\left[(\omega+\epsilon_n^{(0)})\langle\phi_k^{(0)}|\phi_j^{(0)}\rangle - \langle\phi_k^{(0)}|H|\phi_j^{(0)}\rangle\right]z_j^{(1)}(n,\omega+\epsilon_n^{(0)})\\
&\quad= \left[\langle\phi_k^{(0)}|W(\omega)|\phi_j^{(0)}\rangle + \langle\phi_k^{(0)}|H-\epsilon_n^{(0)}|\phi_j^{(1)}(\omega)\rangle\right.\\
&\qquad \left. + \langle\phi_k^{(1)}(-\omega)|H-\epsilon_n^{(0)}|\phi_j^{(0)}\rangle - \omega\langle\phi_k^{(0)}|\phi_j^{(1)}\rangle\right]z_j^{(0)}(n),
\end{aligned} \tag{A10}$$

where we defined the Fourier transform of a generic time-dependent function $f(t)$ by

$$f(t) = \frac{1}{2\pi}\int_{-\infty}^{\infty} f(\omega)\exp[-i\omega t]\,d\omega. \tag{A11}$$

This algebraic equation can be solved for the expansion coefficients $z_j^{(1)}(n,\omega+\epsilon_n)$ either by inversion of the matrix $(\omega+\epsilon_n)\langle\phi_k^{(0)}|\phi_j^{(0)}\rangle - \langle\phi_k^{(0)}|H|\phi_j^{(0)}\rangle$ or by applying a basis transformation to the wave functions $\{\varphi_{n'}^{(0)}\}$ of the static Hamiltonian H. Which of the two approaches is numerically more advantageous depends on the number of basis functions in comparison to the number of bands required to converge the wave function response. In any case, it is quite instructive to apply a basis transformation to the wave functions $\{\varphi_{n'}^{(0)}\}$ of the static Hamiltonian H which yields

$$\begin{aligned}
&\langle\varphi_{n'}^{(0)}|\hat{\varphi}_n^{(1)}(\omega+\epsilon_n)\rangle\\
&\quad= \frac{\langle\varphi_{n'}^{(0)}|W(\omega)|\varphi_n^{(0)}\rangle}{\epsilon_n^{(0)}-\epsilon_{n'}^{(0)}+\omega} + \frac{\langle\varphi_{n'}^{(0)}|H-\epsilon_{n'}^{(0)}|\tilde{\varphi}_n^{(1)}(\omega)\rangle}{\epsilon_n^{(0)}-\epsilon_{n'}^{(0)}+\omega}\\
&\qquad + \frac{\langle\tilde{\varphi}_{n'}^{(1)}(-\omega)|H-\epsilon_n^{(0)}|\varphi_n^{(0)}\rangle}{\epsilon_n^{(0)}-\epsilon_{n'}^{(0)}+\omega} - \langle\varphi_{n'}^{(0)}|\tilde{\varphi}_n^{(1)}(\omega)\rangle.
\end{aligned} \tag{A12}$$

The complete first order change of the wave function is then given by

$$\varphi_n^{(1)}(\mathbf{r},t) = \frac{1}{2\pi}\int_{-\infty}^{\infty}\varphi_n^{(1)}(\mathbf{r},\omega)\exp[-i(\omega+\epsilon_n)t]\,d\omega \tag{A13}$$

with

$$\begin{aligned}
\varphi_n^{(1)}(\mathbf{r},\omega) = \sum_{n'}&\left[\frac{\langle\varphi_{n'}^{(0)}|W(\omega)|\varphi_n^{(0)}\rangle}{\epsilon_n^{(0)}-\epsilon_{n'}^{(0)}+\omega} + \frac{\langle\varphi_{n'}^{(0)}|H-\epsilon_{n'}^{(0)}|\tilde{\varphi}_n^{(1)}(\omega)\rangle}{\epsilon_n^{(0)}-\epsilon_{n'}^{(0)}+\omega}\right.\\
&\left. + \frac{\langle\tilde{\varphi}_{n'}^{(1)}(-\omega)|H-\epsilon_n^{(0)}|\varphi_n^{(0)}\rangle}{\epsilon_n^{(0)}-\epsilon_{n'}^{(0)}+\omega}\right]\varphi_{n'}^{(0)}(\mathbf{r})\\
&+\tilde{\varphi}_n^{(1)}(\mathbf{r},\omega) - \sum_{n'}\langle\varphi_{n'}^{(0)}|\tilde{\varphi}_n^{(1)}(\omega)\rangle\varphi_{n'}^{(0)}(\mathbf{r}).
\end{aligned} \tag{A14}$$

The wave-function response, Eq. (A14), comprises the sum-over-states (SOS) term of conventional perturbation theory,

Pulay terms that correct for deviations of the state $\varphi_n^{(0)}$ and $\varphi_{n'}^{(0)}$, respectively, from the true eigenstate of H, and the basis response (BR) term. The latter consists of the basis response $\tilde{\varphi}_n^{(1)}(\mathbf{r},\omega)$ and a double-counting correction. The Pulay and BR term together constitute the IBC. In Eq. (10) the Pulay term, correcting for deviations of the state $\varphi_n^{(0)}$ from the true eigenstate of H, has been neglected, since we found that this term is usually negligibly small for an occupied state φ_n.

APPENDIX B: CORE ELECTRON RESPONSE

In the LAPW approach, the core-electron wave functions are given as solutions to an atomic Dirac equation. For the calculation of the core-electron response, however, we apply the scalar-relativistic approximation. For notational simplicity we resort to the nonrelativistic Schrödinger equation in the following.

The core-electron wave functions of atom a are given as solutions of

$$\left(H - \epsilon_{lmp}^a\right)\varphi_{lmp}^a(\mathbf{r}) = 0\,, \tag{B1}$$

where only the spherical potential is taken into account in the Hamiltonian H. Due to the atomic boundary conditions, solutions of Eq. (B1) exist only at specific eigenenergies ϵ_{plm}^a. Since the potential is restricted to be spherical, the eigenvalues are degenerate with respect to the magnetic quantum number m ($\epsilon_{lmp}^a = \epsilon_{lp}^a$), and the core wave functions are simply given by

$$\varphi_{lmp}^a(\mathbf{r}) = u_{lp}^a(r)Y_{lm}(\hat{\mathbf{r}})\,, \tag{B2}$$

where p denotes the principal quantum number, l is the angular momentum, and m is the magnetic quantum number.

The first-order change of the core wave function $\varphi_{lmp}^{a(1)}(\mathbf{r},\omega)e^{-i\omega t}$ caused by the perturbation $M_I(\mathbf{r})e^{-i\omega t}$ with $M_I(\mathbf{r}) = M_{LP}^a(r)Y_{LM}(\hat{\mathbf{r}})$ results from a Sternheimer equation formally equivalent to Eq. (5). In contrast to the LAPW basis, however, the solution of the Sternheimer equation for the core electrons has to obey atomic boundary conditions, which makes the solution of the Sternheimer equation unique.

In order to solve this equation numerically, an extended radial mesh that exceeds the MT sphere of atom a is used. In principle, we can employ the same shooting technique as described in our previous paper [20], in which the homogeneous and inhomogeneous Sternheimer equation is integrated outward and inward up to a matching point. The inward integration starts at a large distance from the atomic nucleus. The two homogeneous solutions obtained by inward and outward integration are added in the respective region such that the solution becomes continuous in value and slope at the matching point. In this way, a unique solution is obtained.

However, we observed that for large imaginary frequencies this approach becomes numerically unstable, since for large frequencies the radial part of the homogeneous solution starts to grow exponentially. Hence, we make use of a finite-difference approach, which has the benefit that the explicit computation of the homogeneous solution is completely avoided. The second radial derivative of Eq. (5) is therefore calculated from the finite difference

$$\frac{\partial^2}{\partial r^2} f(r)|_{r=r_k} = \frac{f_{k+1} - 2f_k + f_{k-1}}{(r_{k+1} - r_k)(r_k - r_{k-1})}\,, \tag{B3}$$

with which the Sternheimer equation turns into a set of coupled linear equations of the form $\mathbf{Ax} = \mathbf{b}$. In the case of the Schrödinger equation (scalar-relativistic Schrödinger equation) the corresponding matrix $\mathbf{A}$ has tridiagonal (penta-diagonal) form. For the solution of the algebraic system of band matrix form efficient algorithms exist (e.g., the Thomas algorithm [52]). The atomic boundary conditions can be easily incorporated in the matrix $\mathbf{A}$ by setting $A_{12} = A_{nn-1} = 0$. We validated our implementation by comparing the resulting core-electron response with the one obtained by the shooting method. As long as the shooting method is stable, the results of both approaches are identical.

As an example, we show in Fig. 4 the response of the Ba 4s core state of rocksalt BaO due to a given spherical

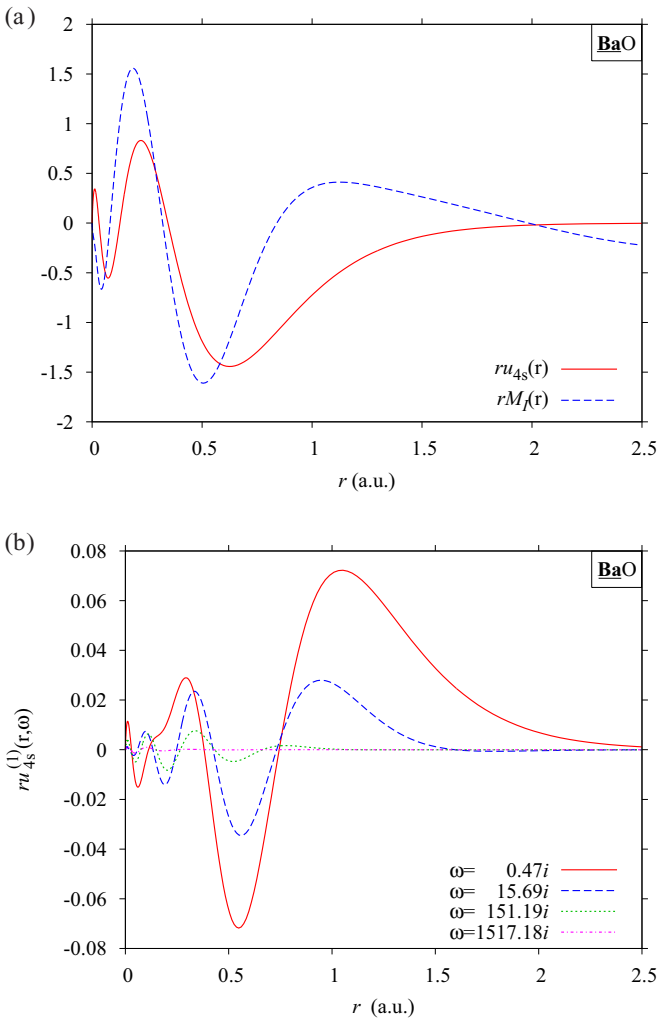

FIG. 4. (Color online) Ba 4s core state of BaO [(red) solid line in (a)] is perturbed by the spherical mixed product basis function shown as the (blue) dashed line in (a). The response of the Ba 4s core is shown for four different imaginary frequencies in (b).

muffin-tin mixed-product-basis function [shown in Fig. 4(a) as the (blue) dashed curve] for different imaginary frequencies. With increasing frequency the radial response is constricted to a smaller and smaller region around the atomic nuclei ($r = 0$), and at the same time the amplitude of the response becomes smaller and smaller.

APPENDIX C: POLARIZABILITY

By utilizing the expression for the first-order change of the wave function [Eq. (A14)], the response function [Eq. (12)] decomposes into a SOS, BR, and Pulay part. The explicit expressions for each of these terms is given in the following:

$$\chi_{IJ}^{\mathrm{SOS}}(\mathbf{q},\omega) = \sum_{\mathbf{k}}^{\mathrm{BZ}} \sum_{n}^{\mathrm{occ.}} \sum_{n'}^{\mathrm{unocc.}} \langle M_I^{\mathbf{q}} \varphi_{n\mathbf{k}} | \varphi_{n'\mathbf{k}+\mathbf{q}} \rangle \langle \varphi_{n'\mathbf{k}+\mathbf{q}} | \varphi_{n\mathbf{k}} M_J^{\mathbf{q}} \rangle \left[\frac{1}{\epsilon_{n\mathbf{k}} - \epsilon_{n'\mathbf{k}+\mathbf{q}} + \omega} + \frac{1}{\epsilon_{n\mathbf{k}} - \epsilon_{n'\mathbf{k}+\mathbf{q}} - \omega} \right] \tag{C1}$$

$$\chi_{IJ}^{\mathrm{BR}}(\mathbf{q},\omega) = \sum_{\mathbf{k}}^{\mathrm{BZ}} \sum_{n}^{\mathrm{occ.}} \langle M_I^{\mathbf{q}} \varphi_{n\mathbf{k}} | \tilde{\varphi}^{(1)}_{n\mathbf{k},J\mathbf{q}}(\omega) + \tilde{\varphi}^{(1)}_{n\mathbf{k},J\mathbf{q}}(-\omega) \rangle - \sum_{\mathbf{k}}^{\mathrm{BZ}} \sum_{n}^{\mathrm{occ.}} \sum_{n'} \langle M_I^{\mathbf{q}} \varphi_{n\mathbf{k}} | \varphi_{n'\mathbf{k}+\mathbf{q}} \rangle \langle \varphi_{n'\mathbf{k}+\mathbf{q}} | \tilde{\varphi}^{(1)}_{n\mathbf{k},J\mathbf{q}}(\omega) + \tilde{\varphi}^{(1)}_{n\mathbf{k},J\mathbf{q}}(-\omega) \rangle \tag{C2}$$

$$\begin{aligned} \chi_{IJ}^{\mathrm{Pulay}}(\mathbf{q},\omega) = \sum_{\mathbf{k}}^{\mathrm{BZ}} \sum_{n}^{\mathrm{occ.}} \sum_{n'} \langle M_I^{\mathbf{q}} \varphi_{n\mathbf{k}} | \varphi_{n'\mathbf{k}+\mathbf{q}} \rangle \Bigg[& \frac{\langle \varphi_{n'\mathbf{k}+\mathbf{q}} | H - \epsilon_{n'\mathbf{k}+\mathbf{q}} | \tilde{\varphi}^{(1)}_{n\mathbf{k},J\mathbf{q}}(\omega) \rangle}{\epsilon_{n\mathbf{k}} - \epsilon_{n'\mathbf{k}+\mathbf{q}} + \omega} + \frac{\langle \varphi_{n'\mathbf{k}+\mathbf{q}} | H - \epsilon_{n'\mathbf{k}+\mathbf{q}} | \tilde{\varphi}^{(1)}_{n\mathbf{k},J\mathbf{q}}(-\omega) \rangle}{\epsilon_{n\mathbf{k}} - \epsilon_{n'\mathbf{k}+\mathbf{q}} - \omega} \\ & + \frac{\langle \tilde{\varphi}^{(1)}_{n'\mathbf{k}+\mathbf{q},J\mathbf{q}}(-\omega) | H - \epsilon_{n\mathbf{k}} | \varphi_{n\mathbf{k}} \rangle}{\epsilon_{n\mathbf{k}} - \epsilon_{n'\mathbf{k}+\mathbf{q}} + \omega} + \frac{\langle \tilde{\varphi}^{(1)}_{n'\mathbf{k}+\mathbf{q},J\mathbf{q}}(\omega) | H - \epsilon_{n\mathbf{k}} | \varphi_{n\mathbf{k}} \rangle}{\epsilon_{n\mathbf{k}} - \epsilon_{n'\mathbf{k}+\mathbf{q}} - \omega} \Bigg]. \end{aligned} \tag{C3}$$

According to our experience the Pulay terms comprising $H - \epsilon_{n\mathbf{k}} | \varphi_{n\mathbf{k}} \rangle$ are negligibly small and can be discarded. Note that if the quantity $\tilde{\varphi}^{(1)}_{n\mathbf{k},J\mathbf{q}}(\omega)$ occurs in the bra only the wave function has to be complex conjugated and not the perturbation, i.e., $\langle \tilde{\varphi}^{(1)}_{n\mathbf{k},J\mathbf{q}}(\omega)|$ corresponds to the response of $\tilde{\varphi}^{\sigma *}_{n\mathbf{k}}$ due to $M_J^{\mathbf{q}}(\mathbf{r}) e^{-i\omega t}$.

[1] W. Kohn and L. J. Sham, Phys. Rev. **140**, A1133 (1965).
[2] *A Primer in Density Functional Theory*, Vol. 620 of *Lecture Notes in Physics*, edited by C. Fiolhais, F. Nogueira, and M. A. L. Marques (Springer, Heidelberg, 2003).
[3] L. Hedin, Phys. Rev. **139**, A796 (1965).
[4] W. G. Aulbur, L. Jönsson, and J. W. Wilkins, Solid State Phys. **54**, 1 (1999).
[5] F. Aryasetiawan and O. Gunnarsson, Rep. Prog. Phys. **61**, 237 (1998).
[6] D. C. Langreth and J. P. Perdew, Solid State Commun. **17**, 1425 (1975).
[7] D. C. Langreth and J. P. Perdew, Phys. Rev. B **15**, 2884 (1977).
[8] A. Hesselmann and A. Görling, Mol. Phys. **109**, 2473 (2011).
[9] H. Eshuis, J. E. Bates, and F. Furche, Theor. Chem. Acc. **131**, 1 (2012).
[10] X. Ren, P. Rinke, C. Joas, and M. Scheffler, J. Mater. Sci. **47**, 7447 (2012).
[11] F. Bruneval and X. Gonze, Phys. Rev. B **78**, 085125 (2008).
[12] O. V. Gritsenko and E. J. Baerends, Phys. Rev. A **64**, 042506 (2001).
[13] F. Della Sala and A. Görling, J. Chem. Phys. **115**, 5718 (2001).
[14] S. Kümmel and L. Kronik, Rev. Mod. Phys. **80**, 3 (2008), and references therein.
[15] A. Görling, J. Chem. Phys. **123**, 062203 (2005).
[16] J. A. Berger, L. Reining, and F. Sottile, Phys. Rev. B **82**, 041103(R) (2010).
[17] J. A. Berger, L. Reining, and F. Sottile, Eur. Phys. J. B **85**, 326 (2012).
[18] R. M. Sternheimer, Phys. Rev. **96**, 951 (1954); **107**, 1565 (1957); **115**, 1198 (1959); **183**, 112 (1969).
[19] M. Betzinger, C. Friedrich, A. Görling, and S. Blügel, Phys. Rev. B **85**, 245124 (2012).
[20] M. Betzinger, C. Friedrich, and S. Blügel, Phys. Rev. B **88**, 075130 (2013).
[21] E. Wimmer, H. Krakauer, M. Weinert, and A. J. Freeman, Phys. Rev. B **24**, 864 (1981).
[22] M. Weinert, E. Wimmer, and A. J. Freeman, Phys. Rev. B **26**, 4571 (1982).
[23] H. J. F. Jansen and A. J. Freeman, Phys. Rev. B **30**, 561 (1984).
[24] D. J. Singh and L. Nordstrom, *Planewaves, Pseudopotentials and the LAPW Method* (Springer Verlag, Berlin, 2006).
[25] S. Y. Savrasov, Phys. Rev. Lett. **81**, 2570 (1998).
[26] H. L. Skriver, *The LMTO method* (Springer, New York, 1984).
[27] M. Methfessel, M. van Schilfgaarde, and R. Casali, in *Electronic Structure and Physical Properties of Solids*, edited by H. Dreysse, Vol. 535 of Lecture Notes in Physics (Springer, Berlin Heidelberg, 2000), pp. 114–147.
[28] P. Pulay, Molec. Phys. **17**, 197 (1969).
[29] F. Aryasetiawan and O. Gunnarsson, Phys. Rev. B **49**, 16214 (1994).
[30] C. Friedrich, A. Schindlmayr, and S. Blügel, Comput. Phys. Commun. **180**, 347 (2009).
[31] M. Betzinger, C. Friedrich, and S. Blügel, Phys. Rev. B **81**, 195117 (2010).
[32] C. Friedrich, S.B lügel, and A. Schindlmayr, Phys. Rev. B **81**, 125102 (2010).
[33] D. Singh, Phys. Rev. B **43**, 6388 (1991).
[34] E. E. Krasovskii, A. N. Yaresko, and V. N. Antonov, J. Electron Spectrosc. Relat. Phenom. **68**, 157 (1994).
[35] C. Friedrich, A. Schindlmayr, S. Blügel, and T. Kotani, Phys. Rev. B **74**, 045104 (2006).
[36] E. E. Krasovskii, Phys. Rev. B **56**, 12866 (1997).
[37] P. E. Blöchl, Phys. Rev. B **50**, 17953 (1994).
[38] G. Kresse and D. Joubert, Phys. Rev. B **59**, 1758 (1999).

[39] J. Rath and A. J. Freeman, Phys. Rev. B **11**, 2109 (1975).
[40] S. L. Adler, Phys. Rev. **126**, 413 (1962).
[41] N. Wiser, Phys. Rev. **129**, 62 (1963).
[42] B.-C. Shih, Y. Xue, P. Zhang, M. L. Cohen, and S. G. Louie, Phys. Rev. Lett. **105**, 146401 (2010).
[43] J. P. Perdew, K. Burke, and M. Ernzerhof, Phys. Rev. Lett. **77**, 3865 (1996); **78**, 1396 (1997).
[44] M. Betzinger, C. Friedrich, S. Blügel, and A. Görling, Phys. Rev. B **83**, 045105 (2011).
[45] M. S. Hybertsen and S. G. Louie, Phys. Rev. B **34**, 5390 (1986).
[46] W. Kang and M. S. Hybertsen, Phys. Rev. B **82**, 195108 (2010).
[47] R. J. Zollweg, Phys. Rev. **111**, 113 (1958).
[48] G. A. Saum and E. B. Hensley, Phys. Rev. **113**, 1019 (1959).
[49] M. Betzinger, C. Friedrich, and S. Blügel (unpublished).
[50] F. Jensen, *Introduction to Computational Chemistry*, 2nd ed. (John Wiley & Sons, Ltd., New York, 2007).
[51] J. Deslippe, G. Samsonidze, M. Jain, M. L. Cohen, and S. G. Louie, Phys. Rev. B **87**, 165124 (2013).
[52] W. H. Press, S. A. Teukolsky, W. T. Vetterling, and B. P. Flannery, *Numerical Recipes 3rd Edition: The Art of Scientific Computing* (Cambridge University Press, New York, 2007).